Advanced Powder Technology 24 (2013) 154–159

Contents lists available at SciVerse ScienceDirect

Advanced Powder Technology

journal homepage: www.elsevier.com/locate/apt

Original Research Paper

Nanocrystalline $LaMnO_3$ preparation and kinetics of crystallization process

Wu Wenwei *, Cai Jinchao, Wu Xuehang, Liao Sen, Wang Kaituo, Tao Lin

School of Chemistry and Chemical Engineering, Guangxi University, Nanning 530004, PR China

ARTICLE INFO

Article history:
Received 3 January 2012
Received in revised form 29 March 2012
Accepted 9 April 2012
Available online 22 April 2012

Keywords:
$LaMnO_3$
Non-isothermal kinetics
Crystallization process
Solid-state reaction at low heat

ABSTRACT

Precursor of nanocrystalline $LaMnO_3$ was synthesized by solid-state reaction at low heat using $La(NO_3)_3{\cdot}6H_2O$, $MnSO_4{\cdot}H_2O$, and $Na_2CO_3{\cdot}10H_2O$ as raw materials. XRD analysis showed that precursor was a mixture containing orthorhombic $La_2(CO_3)_3{\cdot}8H_2O$ and rhombohedral $MnCO_3$. When the precursor was calcined at 800 °C for 2 h, pure phase $LaMnO_3$ with rhombohedral structure was obtained. Magnetic characterization indicated that rhombohedral $LaMnO_3$ behaved weak magnetic properties. The thermal process of the precursor experienced four steps, which involved the dehydration of crystallization water at first, and then decomposition of manganese carbonate into MnO_2, and decomposition of $La_2(CO_3)_3$ and MnO_2 together into $La_2O_2CO_3$ and Mn_2O_3, and lastly reaction of monoclinic $La_2O_2CO_3$ with Mn_2O_3 and formation of rhombohedral $LaMnO_3$. Based on the Kissinger equation, the value of the activation energy associated with the formation of rhombohedral $LaMnO_3$ was determined to be 260 kJ mol^{-1}. The value of the Avrami exponent, n, was equal to 1.68, which suggested that crystallization process of $LaMnO_3$ was the random nucleation and growth of nuclei reaction.

1. Introduction

Lanthanum manganites ($LaMnO_3$) with perovskite structure has many unique properties, such as low Neel temperature ($T_N \sim 480$ K), antiferromagnetic properties, insulation [1]. Alkali metals and alkali earth metals substitution for La lead to many interesting properties such as metallicity, ferromagnetism, and charge ordering [2–5]. These excellent properties make $LaMnO_3$ suitable for many applications in the field of solid oxide fuel cells [6], giant magneto resistance [3], catalysts [7,8], etc.

Since $LaMnO_3$ was proposed, various methods have been developed to synthesize crystalline $LaMnO_3$ compounds, including refluxing route [1], mechanochemical synthesis, solid-state reaction at high temperature [9], co-precipitation [10], polymeric gel [11], hydrothermal treatment [12], and sol–gel synthesis [13,14], etc. It was found that crystallite diameter and crystalline phases of $LaMnO_3$ associated with its properties were highly dependent on the synthesis and processing methods. Such as, Daundkar et al. [1] obtained crystalline $LaMnO_3$ by refluxing route. Zhang et al. [9] obtained pure phase $LaMnO_3$ by mechanochemical synthesis after long milling time. Li et al. [14] synthesized $LaMnO_3$ by sol–gel process. However, these processes mentioned above were not easy to obtain pure phase $LaMnO_3$. Therefore, new synthesis methods for $LaMnO_3$ still need to be studied and innovated further. Besides, the kinetics study of crystallization for $LaMnO_3$ is needed to obtain high-quality crystalline $LaMnO_3$ for practical applications.

In this paper, rhombohedral $LaMnO_3$ was synthesized via thermal decomposition of Mn^{2+} and La^{3+} carbonate mixture in air, and kinetics of the crystallization and magnetic properties of $LaMnO_3$ were investigated. Non-isothermal kinetics of the crystallization process of $LaMnO_3$ was interpreted by the Kissinger method [15–17]. Avrami exponent, n, was used to estimate mechanism of crystallization process.

2. Experimental

2.1. Reagent and apparatus

All chemicals were of reagent grade purity (>99.9%). Thermogravimetry and differential scanning calorimetry (TG/DSC) measurements were made using a Netsch 40PC thermogravimetric analyzer. X-ray powder diffraction (XRD) was performed using a Rigaku D/max 2500 V diffractometer equipped with a graphite monochromator and a Cu target. The FT-IR spectra of the precursor and its calcined products were recorded on a Nexus 470 FT-IR instrument. The morphology of the calcined samples and energy dispersive X-ray spectrometer (EDS) were obtained on S-3400 scanning electron microscopy. The specific magnetizations of the calcined sample powders were carried out at room temperature using a magnetic property measurement system (SQUID-MPMS-XL-5).

* Corresponding author.
E-mail address: gxuwuwenwei@yahoo.com.cn (W. Wenwei).

0921-8831/$ - see front matter © 2012 The Society of Powder Technology Japan. Published by Elsevier B.V. and The Society of Powder Technology Japan. All rights reserved.
http://dx.doi.org/10.1016/j.apt.2012.04.004

2.2. Preparation of nanocrystalline $LaMnO_3$

The $LaMnO_3$ precursor was prepared by solid-state reaction at low heat [18,19] using $La(NO_3)_3{\cdot}6H_2O$, $MnSO_4{\cdot}H_2O$, and $Na_2CO_3{\cdot}10H_2O$ as starting materials. In a typical synthesis, $La(NO_3)_3{\cdot}6H_2O$ (35.81 g), $MnSO_4{\cdot}H_2O$ (13.98 g), $Na_2CO_3{\cdot}10H_2O$ (70.99 g), and surfactant polyethylene glycol (PEG)-400 (3.0 mL, 50 vol.%) were put in a mortar, and the mixture was fully ground by hand with a rubbing mallet for 40 min. The grinding velocity was about 100 circles/min, and the strength applied was moderate. The reactant mixture gradually became damp, and then a paste formed quickly. The reaction mixture was kept at 30 °C for 1 h. The mixture was washed with deionized water to remove soluble inorganic salts until SO_4^{2-} ion could not be visually detected with a 0.5 mol L^{-1} $BaCl_2$ solution. The solid was then washed with a small amount of anhydrous ethanol and dried at 75 °C for 3 h. Nanocrystalline $LaMnO_3$ was obtained via calcining the precursor at 800 °C in air for 2 h.

3. Determination of kinetic parameters of crystallization process

According to DSC curves and the Kissinger equation (Eq. (1)) [17], the activation energy of $LaMnO_3$ crystallization process can be obtained.

$$\ln\frac{\beta}{T_P^2} = -\frac{E_a}{RT_P} + \ln\frac{AR}{E_a} \quad (1)$$

where β is the heating rate (K min^{-1}), T_P is the peak temperature (K) in DSC curve, E_a is the activation energy (kJ mol^{-1}) of crystallization process, R is the gas constant (8.314 × 10^{-3} kJ mol^{-1} K^{-1}), and A is the pre-exponential factor. According to Eq. (1), the plot of $\ln(\beta/T_P^2)$ versus $1/T_P$ can be obtained by a linear regression of least-square method. The dependence of $\ln(\beta/T_P^2)$ on $1/T_P$ must give a good linear relation. Thus, reaction activation energy E_a can be obtained from linear slope ($-E_a/R$), and the pre-exponential factor A can be obtained from linear intercept ($\ln(AR/E_a)$).

4. Results and discussion

4.1. TG/DSC analysis of the precursor

Fig. 1 showed the TG/DSC curves of the precursor at four heating rates of 10, 15, 20, and 23 K min^{-1} from 38 to 945 °C. The TG/DSC curves showed that the thermal process of the $LaMnO_3$ precursor below 945 °C experienced four steps. For heating rate of 10 K min^{-1}, the first step starts at about 50 °C, ends at 148 °C, and characterized by an endothermic DSC peak at about 105 °C, which can be attributed to dehydration of the eight crystal water molecules from $La_2(CO_3)_3{\cdot}2MnCO_3{\cdot}8H_2O$ and the formation of $La_2(CO_3)_3{\cdot}2MnCO_3$. The observed mass loss in the TG curve was 18.03%, which was in good agreement with 17.33% theoretic mass loss of dehydration of the eight crystal water molecules from $La_2(CO_3)_3{\cdot}2MnCO_3{\cdot}8H_2O$. The second decomposition step begins at 148 °C, and ends at 316 °C, which involves a weak endothermic DSC peak at about 316 °C, attributed to the decomposition of $La_2(CO_3)_3{\cdot}2MnCO_3$ into $La_2(CO_3)_3$ and MnO_2 in air. The observed mass loss in the TG curve was 6.67%, which was in good agreement with 6.73% theoretic mass loss of reaction of $La_2(CO_3)_3{\cdot}2MnCO_3$ with one O_2 molecule, and of two CO_2 molecules. The third step thermal decomposition begins at 316 °C, and ends at 483 °C, which involves a stronger endothermic DSC peak at about 444 °C, attributed to the decomposition of $La_2(CO_3)_3$ and MnO_2 into $La_2O_2CO_3$ and Mn_2O_3 in air [20]. The observed mass loss in the TG curve was 11.97%, which was in good agreement with 12.5% theoretic mass loss of decomposition of $La_2(CO_3)_3{\cdot}2MnO_2$, and of two CO_2 molecules and a half O_2 molecule. The fourth step decomposition starts at 483 °C, and ends at about 779 °C, characterized by a weak exothermic DSC peak at about 738 °C. The observed mass loss in the TG curve was 5.03%, which was close to 5.29% theoretic mass loss of reaction of $La_2O_2CO_3$ with Mn_2O_3, and off one CO_2 molecule. No other endothermic DSC peak that was ascribed to decomposition of $La_2O_2CO_3$ above 600 °C, which indicated that endothermic DSC peak of decomposition of $La_2O_2CO_3$ was overlapped with exothermic DSC peak of crystallization process of $LaMnO_3$, and exothermic heat effect was greater than endothermic heat effect. The peak temperature of crystallization process of $LaMnO_3$ is the temperature at which it attains its maximum. From Fig. 1b, there was an upward shift in T_P with increasing heating rate, peak temperatures from heating rate of 10, 15, 20, and 23 K min^{-1} were 737, 748, 757, and 766 °C.

4.2. IR spectroscopic analysis of the precursor and its calcined samples

The FT-IR spectra of the precursor and its calcined samples were shown in Fig. 2. The precursor exhibited a strong and broad band at 3384 cm^{-1} that can be assigned to stretching vibrations in water of crystallization. The weak band at about 742 cm^{-1} was attributed to the water libration (hindered rotation). The weak band, which appears at 1655 cm^{-1} in the spectrum of the precursor, can be ascribed to the bending mode of the HOH [15,16]. The bands at 2350, 1478, and 1381 cm^{-1} can be assigned to either the appearance of M–OCO_2 (M = La, Mn) bonds and/or to the combinations

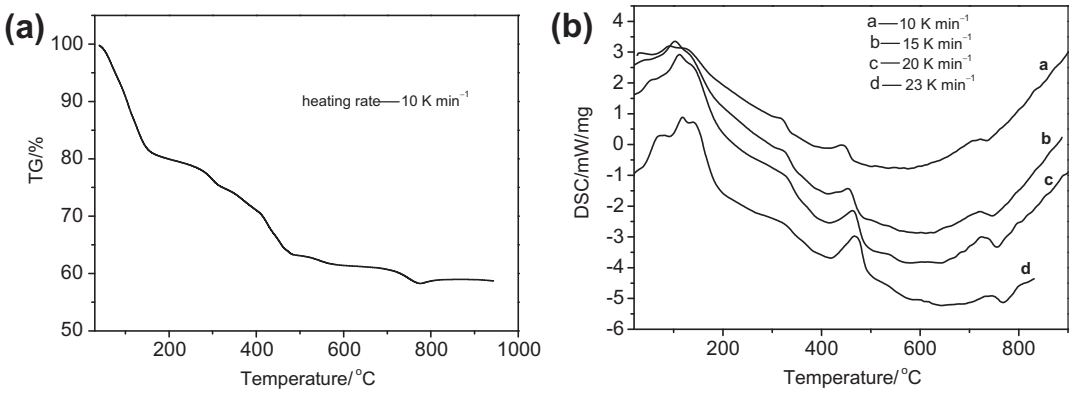

Fig. 1. TG/DSC curves of the $LaMnO_3$ precursor: (a) TG analysis; (b) DSC analysis.